



Anti-microbial and Anti-inflammatory Studies of Zinc-Salen Complex



Asemave K.^{1*}, Edward T.², Atime Iningev S.T.³ & Agber C.⁴

^{1,2,3,4}Dept. Chemistry, Rev. Fr. Moses Orshio Adasu University, Makurdi – Nigeria

*Corresponding Author Email: kasemave@gmail.com

ABSTRACT

There is much traction about Schiff base metal complexes because of their structural versatility, potentials in bioactivities etc. Thus, N,N'-bis(salicylidene)ethylenediamine - a salen ligand- was synthesized from salicylaldehyde and ethylenediamine; then followed by coordination with zinc(II) to form a Zn-salen complex. The yields of the salen and its zinc complex were $81 \pm 2\%$ and $73 \pm 2\%$, respectively. These samples were characterized by melting/decomposition point analyses, solubility tests, Fourier-transform infrared (FTIR) and UV-Visible absorptions. From the results of FTIR, there were evidence for azomethine linkage and Zn complexation because of the characteristic shift of the C=N stretching vibration and deprotonation of the phenolic O-H group. UV-Visible analyses showed $\pi \rightarrow \pi^*$ and $n \rightarrow \pi^*$ transitions of the salen, along with a salen-to-metal charge transfer band in the Zn-salen complex at 350 – 420 nm. These are reasonable features implying coordination between the Zn ion and the base. Melting point of $128 \pm 2^\circ\text{C}$ for the salen ligand was obtained, indicating high purity. On the otherhand, the Zn-salen complex showed lower melting point as compared to other reported analogues. The Zn-salen was lipophilic than the free salen based on the solubility results. The Zn-salen complex gave generic antibacterial activities against Gram-positive, Gram-negative, and fungal strains. In vitro anti-inflammatory assessment showed moderate COX-1 and COX-2 inhibition. And Zn-salen gave higher COX-2 selectivity compared to ibuprofen. These findings implied Zn-salen has potential for the development of novel antimicrobial and anti-inflammatory agents, necessitating detail pharmacological investigations.

Keywords:

Metal-Ligand Complex,
Biological Assay

INTRODUCTION

Metal-ligand complexes generally have peculiar; structural versatility, electronic configuration, biological properties etc, hence are quite important in Medicinal field in particular and Chemistry in general. Thus, Schiff Bases (derived from the condensation of amines with aldehydes/ketones (Musa et al., 2025; Rajasekar et al., 2025), have become seriously attractive due to structural robustness, strong metal-binding ability and their potential applications (Jain et al., 2023). These compounds are known for their antimicrobial, anti-inflammatory, antiviral, and anticancer activities (Raju et al., 2022). Now, salen is a Schiff Base obtained from salicylaldehyde and diamines with tetradentate architecture. They form stable complexes with various metals by two imine nitrogen atoms and two phenolic oxygen atoms (Hui et al., 2022). In addition, metal-salen complexes like other coordination compounds do express enhanced biological activity than the free ligands (Elghamry et al., 2022; Mangamamba et al., 2014).

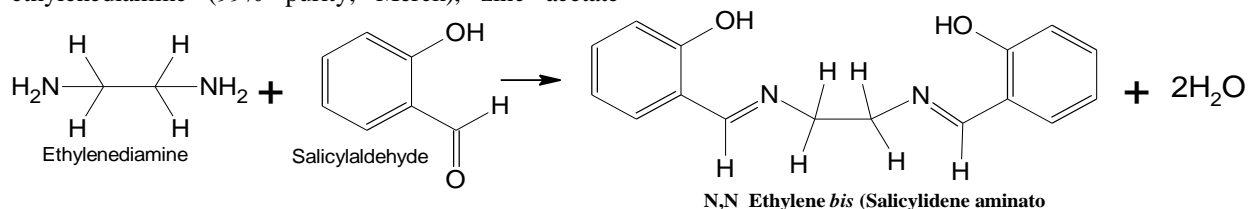
In fact, the zinc-salen complex is essential because zinc is relatively less harmful and biologically crucial metal that is involved in immune function, wound healing, and inflammation regulation (Sharma et al., 2021). When zinc bonds to salen it can alter the ligand's electronic configuration, lipophilicity, and solubility, leading to increased interphase with microbial cell membranes and inflammation-causing enzymes (Al-Farraj et al., 2025). Zn-salen complexes have shown promising activities against bacteria as well as fungi pathogen. Therefore, due to the increasing global challenge of antimicrobial resistance, such complexes are being considered as potential alternatives to conventional antibiotics (Al-Farraj et al., 2025). Their bioactivities mechanisms stem from DNA interaction, enzyme inhibition, membrane disruption, and the generation of reactive oxygen species. In addition to antipathogenic effects, Zn-salen complexes have anti-inflammatory properties (Sandhu et al., 2023). They can suppress; cyclooxygenase enzymes (COX-1 & COX-2),

protein denaturation, and prostaglandin synthesis, which is a leverage over traditional NSAIDs; often linked with side effects (Singh et al., 2022). The Zn–salen complexes can be characterized by FTIR, UV–Visible spectroscopy, melting point analysis, solubility etc. In addition, antimicrobial and anti-inflammatory assays are some ways of characterizing/applying coordination compounds (Singh et al., 2022). Overall, Zn–salen complexes represent promising candidates for the development of new antimicrobial and anti-inflammatory agents. Therefore, this research investigates the preparation, characterization, and biological properties of a zinc-salen complex, focusing on its anti-inflammatory and antimicrobial potentials.

MATERIALS AND METHODS

Chemicals, Solvents, and Reagents

KBr (spectroscopic grade, Sigma-Aldrich), salicylaldehyde (99% purity, Sigma-Aldrich), methanol (HPLC grade, 99.9% purity, Fisher Scientific), ethylenediamine (99% purity, Merck), zinc acetate



Equation 1: Preparation of Schiff Base Ligand (*N, N'*-bis(salicylidene)ethylenediamine, Salen)

Synthesis of Zinc-Salen Complex

The dried ligand (10 mmol, 2.36 g) was dissolved in methanol (20 mL). Zinc acetate dihydrate (10 mmol, 2.19 g) in methanol (10 mL) was added dropwise with stirring.



Figure 1: The prepared Salen

dihydrate ($\geq 98\%$ purity, Alfa Aesar), bovine serum albumin (BSA, $\geq 96\%$ purity, Sigma-Aldrich), phosphate buffer (prepared from analytical grade monobasic and dibasic sodium phosphate, purity $\geq 99\%$, BDH Chemicals), pH (6.3–6.5), ciprofloxacin, gentamycin, ceftriaxone, and fluconazole, Sterile filter paper disks (6 mm diameter) and nutrient agar (Oxoid), methanol (Fisher Scientific), n-hexane ($\geq 97\%$ purity, Merck), chloroform (HPLC grade, 99.8% purity, BDH), and dimethyl sulfoxide (DMSO, anhydrous, $\geq 99.9\%$ purity, Sigma-Aldrich). PerkinElmer Spectrum BX FTIR spectrophotometer and Shimadzu UV-2600 spectrophotometer.

Synthesis of Schiff Base Ligand (Salen)

Salicylaldehyde (2.13 mL) was dissolved in methanol (15 mL) and ethylenediamine (0.67 mL) was added dropwise with stirring. The mixture was refluxed for 4 h, producing a yellow precipitate, which was filtered, washed with cold methanol, and dried (Vafazadeh & Bagheri, 2015). See Equation 1 and Figure 1. Percent yield is $81 \pm 2\%$

The mixture was refluxed for 1 h, cooled, and the precipitate was filtered and dried (Vafazadeh & Bagheri, 2015). See Figure 2. Percent yield is $73 \pm 2\%$.



Figure 2: The prepared Zn-Salen complex

Solubility Test

The solubility test was performed in selected solvents, namely methanol, n-hexane, chloroform, and dimethyl sulfoxide (DMSO). Approximately 10 mg of each sample was placed separately into clean, dry test tubes. To each

test tube, 2 mL of the solvent was added at r.t. The mixtures were gently agitated and equilibrated by standing for 10 min. Subsequently, visual observations for clarity on the mixtures were made. If a mixture becomes clear, the compound was recorded as soluble;

otherwise it was taken as partially soluble/ insoluble (Asemave, 2016).

Melting/Decomposition Point

The melting/decomposition points of the samples were determined using a melting point apparatus. Small quantity of each sample was packed into separate capillary tubes sealed at one end. The tube was then placed in the melting point apparatus and heated. The temperature range at which the solid first began to melt and completely liquefied was recorded as the melting point of the salen ligand; whereas, for the Zn–salen complex, that was recorded as the decomposition point.

FTIR Absorption

The Fourier Transform Infrared (FTIR) absorptions of the salen ligand and Zn–salen complex were carried out using a PerkinElmer Spectrum BX FTIR spectrophotometer in the range of 4000 - 400 cm^{-1} . KBr pellet method was used for samples preparation. Thus, a small amount of each finely ground sample was completely mixed with KBr and compressed into pellet. The pellets were applied in the sample holder, and the FTIR absorptions were recorded (Asemave et al., 2019).

UV-Visible Absorption

The UV–Visible absorptions of the salen ligand and its complex were recorded using a UV–Visible spectrophotometer. About 1×10^{-5} M each of the samples were prepared in methanol. The absorbances recorded over the wavelength range of 200–800 nm (Asemave et al., 2012).

Antimicrobial Activity (Disk Diffusion Method)

The disk diffusion method was employed for the antimicrobial studies. The organisms used were *Staphylococcus aureus*, *Escherichia coli*, *Candida albicans*, and *Salmonella typhi*. The samples concentrations were 50 $\mu\text{g/mL}$. For each turn, fresh cultures of the test microorganisms were prepared and inoculated on the agar media to obtain uniform growth.

Thereafter, solution of the Zn–salen complex was put on the sterile paper disks and placed on the inoculated agar plates. Ciprofloxacin, gentamycin, ceftriaxone and fluconazole were used as the standards. On the otherhand, the negative control composed of solvent-loaded disk. All the plates were equilibrated at 37 °C for 24 h and 28–30 °C for 48 h, for bacterial and fungal species respectively. Subsequently, the zones of inhibition around the disks were measured and recorded (Haruna et al., 2023).

Anti-Inflammatory Activity (Albumin Denaturation Assay)

The anti-inflammatory activity of the Zn–salen complex (at 100 μM) in comparison to ibuprofen as the standard drug were investigated. Bovine serum albumin (BSA), phosphate buffer (pH \approx 6.3–6.5), and Zn–salen were mixed. More so, a mixture containing ibuprofen, and also another containing neither Zn–salen nor ibuprofen were prepared to serve as the positive, and negative controls, respectively. The reaction mixtures were conditioned at 37 °C for a fixed period and subsequently heated to trigger protein denaturation. Upon cooling to r.t, the absorbance was measured. Using the absorbances, the IC_{50} values for COX-1 and COX-2 inhibition were calculated. Furthermore, the selectivity index (SI) was determined as the ratio of IC_{50} (COX-1) to IC_{50} (COX-2) (Elnagar et al., 2021).

RESULTS AND DISCUSSION

UV Visible absorption

The results of the UV–Visible experiment (see Figure 3) of the free ligand gave strong ultraviolet absorption bands at; 250–280 nm ($\pi \rightarrow \pi^*$ transitions for the aromatic rings); 300–350 nm (corresponds to $n \rightarrow \pi^*$ transitions of the imine group). These are typical UV-Visible characteristic of Schiff bases such as salen (Sheokand et al., 2023). These bands are in conformity with the formation of the azomethine linkage and extended conjugation in the salen framework. See Figure 3.

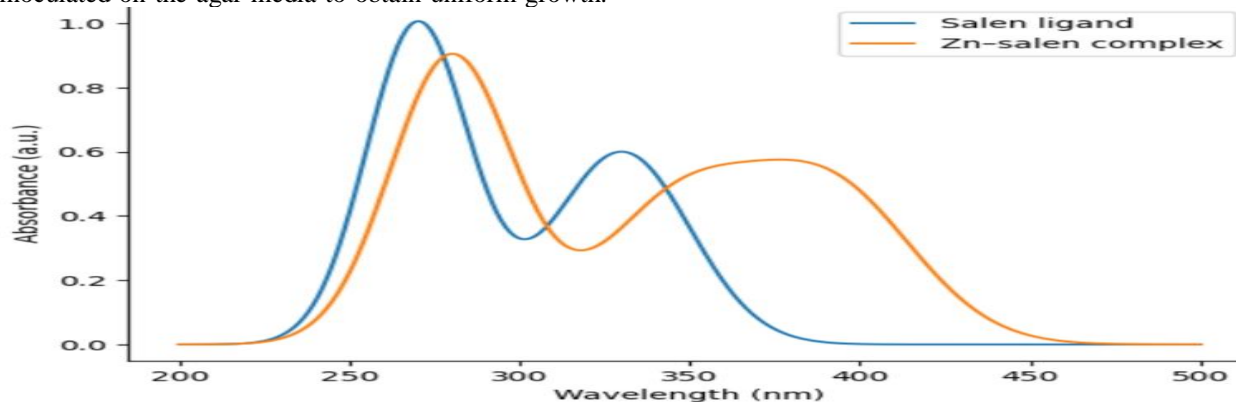


Figure 3: UV Visible Spectra of the salen and Zn-salen

Upon bonding with the Zn(II), the UV–Visible absorption results showed slight red shift of $\pi \rightarrow \pi^*$ transitions due to increased conjugation (Mohammed Ali Mohsen et al., 2024). A new broad band in the 350–420 nm region was observed and assigned to salen-to-Zn charge transfer (Azoogh & Akbarzadeh-Tb, 2025). These imply successful Zn–salen complex formation. The orange-yellow and light-yellow colours of the salen and Zn-salen, respectively are also in support of the UV-Visible results. These colours are due extended π -conjugated system in these structures.

Melting/ Decomposition points

The melting point/ thermal properties of the salen and Zn–salen were investigated. The salen ligand showed a sharp melting point at 128 ± 2 °C with a narrow decomposition range, indicating high purity. This value is in tandem with previous reports of 125–130 °C (Hadjeb et al., 2024; Vafazadeh & Bagheri, 2015). Thermal decomposition temperature of the Zn-salen compound was observed at 279 ± 2 °C (Vafazadeh & Bagheri, 2015). This seems to be lower compared to 3d transition analogues, which decompose at higher temperatures (300–330 °C). This reduced stability may be attributed to weaker Zn–salen interactions and less rigidity of the coordination geometry.

Solubility Results

The free salen ligand was soluble in methanol, chloroform, and DMSO, but insoluble in n-hexane and

water. Its methanol solubility is due to hydrogen bonding with phenolic and amine groups. Similarly, solubility in chloroform arises from dipole–dipole interactions with aromatic rings. DMSO has higher polarity and solvation ability, hence it effectively dissolves the salen ligand. Meanwhile, Zn-salen was only soluble in chloroform and DMSO, and partially soluble in methanol. Partial methanol solubility may entail that zinc bonding lessen ligand polarity or causes steric effects. Upon complexation of the salen by Zn a unique structure/complex with peculiar electronic distribution and molecular geometry is formed. Such complexes are often less hydrophilic than the parent species. This made the Zn-salen soluble in chloroform and DMSO. Therefore, this lipophilicity traits could improve bioavailability and therapeutic applicability.

FTIR Spectra

The results of FTIR spectra/absorptions for the Schiff base and Zn-salen are given in Figures 4, 5 & Table 1). A strong absorption band at 1669.8 cm^{-1} is for the imine (C=N) stretching vibration. This signifies azomethine linkage formation in the Schiff base, salen. In addition, there is absence of a carbonyl peak (1700 cm^{-1}) in Figure 4. It is a proof that there was complete conversion of the aldehyde precursor. A broad band at 3280.1 cm^{-1} is linked to the phenolic O–H stretching. Interestingly, a stretching vibration at 1558 cm^{-1} (C = C) significantly supports the ligand's aromatic structure.

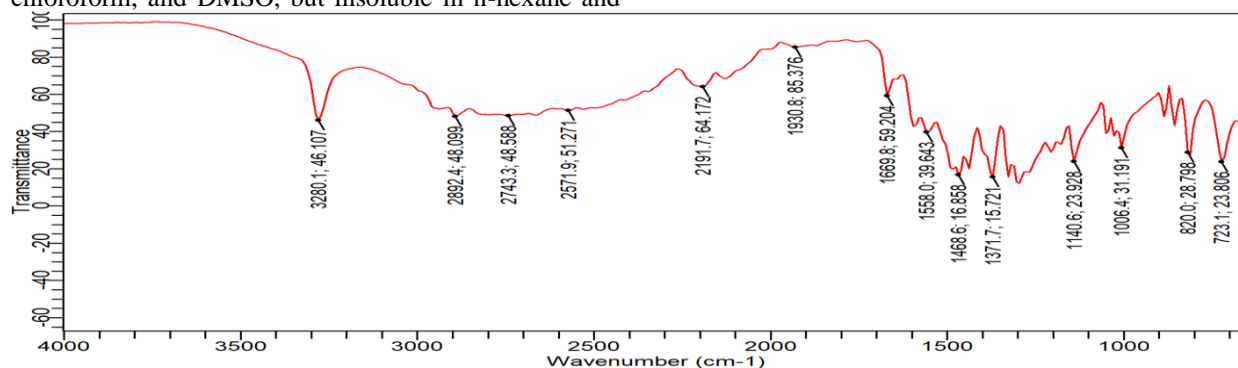


Figure 4: FTIR spectrum of Salen ligand

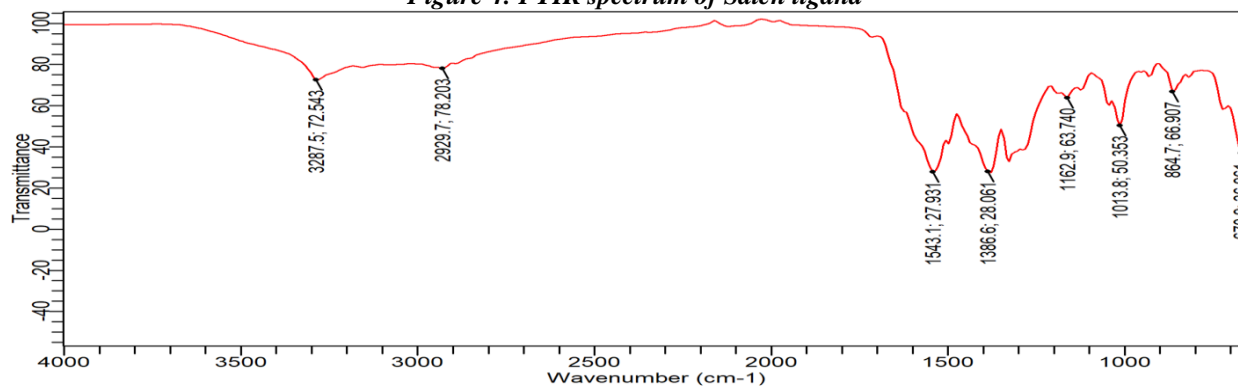
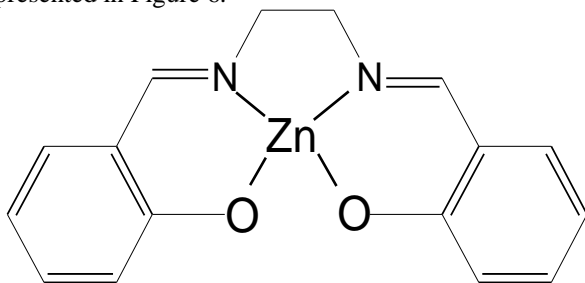


Figure 5: FTIR spectrum of zinc-Salen complex

Table 1: FTIR absorption bands

Functional group	Salen ligand (cm ⁻¹)	Zn-Salen complex (cm ⁻¹)
C=N	1669.8	1543.1
O-H	3280.1 (intense)	3287.5 (very weak)
C=C	1558.0	1543.1
C-O	1371.7	1386.6

The FTIR spectra of the Zn-salen showed that the C=N stretching frequency shifted substantially from 1669.8 cm⁻¹ in the free ligand to 1543.1 cm⁻¹, which is an evidence for bonding between the imine nitrogen to Zn(II). Additionally, the suppression of the phenolic O-H band (3287.5 cm⁻¹) suggests deprotonation and formation of Zn-O bonds (Hadjeb et al., 2024; Vafazadeh & Bagheri, 2015). Although Zn-N vibrations below 670 cm⁻¹ were not observed due to instrumental settings, generally, the spectral changes implied strong evidence for successful Zn-salen complex formation. The geometry could be square planar or slightly distorted tetrahedral. Therefore, the structure of the zn-Salen is presented in Figure 6.

**Figure 6: Structure of the Zn-Salen Complex**

Biological Activity

Antimicrobial and Activities

The Zn-salen complex gave antimicrobial activity against all tested microorganisms (as given in Table 2), with zones of inhibition being highest in *Escherichia coli* (16 mm) and *Staphylococcus aureus* (15 mm); followed by moderate inhibition against *Candida albicans* (14 mm), while *Salmonella typhi* showed the least susceptibility (13 mm). the standard antibiotics and antifungal drugs produced higher inhibition zones. Despite lower strength compared to conventional drugs, the Zn-salen complex exhibits generic antimicrobial and antifungal potentials. Its comparable activity with respect to the standards against, say *E. coli* and *S. aureus* is of much interest given the resistance typically associated with Gram-negative bacterial membranes (Hadjeb et al., 2024).

Table 2: Antimicrobial Activity Data

Microorganism	Complex (mm)	Standard (mm)
<i>S. aureus</i>	15	23 (Ciprofloxacin)

<i>C. albicans</i>	14	21 (Fluconazole)
<i>E. coli</i>	16	22 (Gentamycin)
<i>S. typhi</i>	13	26 (Ceftriaxone)

Table 3: Anti-inflammatory Activity Data

Parameter	Zn-Salen	Ibuprofen
COX-1 IC ₅₀ (μM)	15.3	12.8
COX-2 IC ₅₀ (μM)	8.7	7.9
Selectivity (COX-1/COX-2)	1.76	1.62

Anti-inflammatory Activities

COX-1 protects the gastric lining, whereas, COX-2 is primarily involved in inflammation. Modern anti-inflammatory drug targets exclusive inhibition of COX-2 to reduce gastrointestinal side effects associated to COX-1 inhibition. Zn-salen inhibits COX-1 and COX-2 at 15.3 μM and 8.7 μM, respectively, while ibuprofen shows slightly greater potency with IC₅₀ values of 12.8 μM (COX-1) and 7.9 μM (COX-2). Notwithstanding, selectivity deduced reveals that Zn-salen is more COX-2 selective, with a COX-1/COX-2 IC₅₀ ratio of 1.76 compared to 1.62 for ibuprofen (Haloi et al., 2025). This higher selectivity of Zn-salen entails that the sample preferentially targets inflammatory pathways, but evades the gastroprotective COX-1 enzyme, thus masking gastrointestinal side effects.

CONCLUSION

The paper reports successful preparation of the Schiff base ligand, its zinc (II) complex (Zn-salen) and their characterizations. The sharp melting point of the salen and the thermal behavior of the Zn-salen complex were in harmony with previous knowledge. More so, the spectroscopic evaluations provided evidence of complex formation of Zn-salen. Hence, FTIR absorptions indicated the characteristic imine (C=N) peak in salen. The peak shifted downward in frequency upon zinc complexation; plus, disappearance of the phenolic O-H peak that was originally in the salen. These observations highly suggest tetradentate chelation through nitrogen and oxygen donor atoms. The UV-Visible results also provided evidence of coordination of Zn as bathochromic shifts and salen-to-Zn charge transfer bands were observed. Complex formed has different solubility to salen, potentially increasing its suitability for biological applications. The Zn-salen complex again produced broad-spectrum antimicrobial activities against Gram-positive and Gram-negative bacteria as well as fungal species. It was also observed that the coordinated compound showed promising anti-inflammatory activity with higher COX-2 selectivity than ibuprofen, suggesting a reduced likelihood of gastrointestinal side effects associated with non-selective COX inhibition.

REFERENCE

- Al-Farraj, E. S., Alharbi, S. K., Feizi-Dehnayebi, M., Asghar, B. H., Alahmadi, N., Eskander, T. N. A., Alghamdi, M. A., & Abu-Dief, A. M. (2025). Molecular, Stoichiometric, Stability and Biological Investigations of Novel Multifunctional Salen Metal Chelates: From Synthesis to Therapeutic Potential Supported by Theoretical Approaches. *Applied Organometallic Chemistry*, 39(8). <https://doi.org/10.1002/aoc.70273>
- Asemave, K. (2016). *Biobased Lipophilic Chelating Agents and their Applications in Metals Recovery*. University of York, UK.
- Asemave, K., Byrne, F. P., Clark, J. H., Farmer, T. J., & Hunt, A. J. (2019). Modification of bio-based β -diketone from wheat straw wax: synthesis of polydentate lipophilic super-chelators for enhanced metal recovery. *RSC Advances*, 9(7). <https://doi.org/10.1039/c8ra09426h>
- Asemave, K., Yiase, S. G., & Adejo, S. O. (2012). Kinetics and Mechanism of Substitution Reaction of trans-Dichlorobis (ethylenediammine) cobalt (III) chloride with Cysteine. *Int. J. Modern Org. Chem*, 1(1), 1–9.
- Azoogh, S., & Akbarzadeh-Tb, N. (2025). Preparation of bimetallic Cu, Zn complex with OPD: Synthesis, characterization, spectroscopic methods, and interaction with FS-DNA. *Advanced Journal of Nanochemistry and Medicine*, 1(2), 100–113. <https://doi.org/https://doi.org/10.48309/ajnm.2025.534445.1007>
- El-ghamry, M. A., Elzawawi, F. M., Aziz, A. A. A., Nassir, K. M., & Abu-El-Wafa, S. M. (2022). New Schiff base ligand and its novel Cr(III), Mn(II), Co(II), Ni(II), Cu(II), Zn(II) complexes: spectral investigation, biological applications, and semiconducting properties. *Scientific Reports*, 12(1). <https://doi.org/10.1038/s41598-022-22713-z>
- Elnagar, M. M., Samir, S., Shaker, Y. M., Abdel-Shafi, A. A., Sharmoukh, W., Abdel-Aziz, M. S., & Abou-El-Sherbini, K. S. (2021). Synthesis, characterization, and evaluation of biological activities of new 4'-substituted ruthenium (II) terpyridine complexes: Prospective anti-inflammatory properties. *Applied Organometallic Chemistry*, 35(1). <https://doi.org/10.1002/aoc.6024>
- Hadjeb, R., Hamitouche, H., & Menasra, H. (2024). Experimental and theoretical study of two Salen-type Schiff bases: green synthesis, characterization, corrosion inhibition efficiency, and biological activity. *Digest Journal of Nanomaterials and Biostructures*, 19(3), 1063–1076.
- <https://doi.org/https://doi.org/10.15251/DJNB.2024.193.1063>
- Haloï, P., Mandal, R. K., & Barman, P. (2025). A new fluorinated Schiff base and its Cu(II), Co(II), and Zn(II) complexes: Spectral characterization, DNA binding, in-vitro biological assays and molecular docking study. *Inorganic Chemistry Communications*, 182. <https://doi.org/10.1016/j.inoche.2025.115612>
- Haruna, A., Sirajo, I. T., Rumah, M. M., & Albashir, Y. (2023). Synthesis, Characterization, Biological Properties, ADMET and Drug-likeness Analysis of Mn (II) complexes with Schiff Bases Derived from Sulphathiazole and 4-diethylaminosalicylaldehyde/Salicylaldehyde. *Journal for Research in Applied Sciences and Biotechnology*, 2(6). <https://doi.org/10.55544/jrasb.2.6.10>
- Hui, E. Y. L., Tay, D. W. P., Richard, J. A., Pohancenikova, Z., Renault, K., Romieu, A., & Lim, Y. H. (2022). Structural investigation of Fe(III)-salen complexes as “turn-on” fluorogenic probes for selective detection of pyrophosphate ions. *Dyes and Pigments*, 207. <https://doi.org/10.1016/j.dyepig.2022.110708>
- Jain, S., Rana, M., Sultana, R., Mehendi, R., & Rahisuddin. (2023). Schiff Base Metal Complexes as Antimicrobial and Anticancer Agents. *Polycyclic Aromatic Compounds*, 43(7). <https://doi.org/10.1080/10406638.2022.2117210>
- Mangamamba, T., Ganorkar, M. C., & Swarnabala, G. (2014). Characterization of Complexes Synthesized Using Schiff Base Ligands and Their Screening for Toxicity Two Fungal and One Bacterial Species on Rice Pathogens. *International Journal of Inorganic Chemistry*, 2014. <https://doi.org/10.1155/2014/736538>
- Mohammed Ali Mohsen, E., Saeed, A. A. M., & Alawi Bin Yahia, A. R. (2024). Synthesis, characterization, and bioactivity evaluation of several divalent transition metal ion-bioflavonoid complexes. *Results in Chemistry*, 7. <https://doi.org/10.1016/j.rechem.2024.101535>
- Musa, A., Ibrahim, S. A., & Garba, A. A. (2025). Synthesis, Characterization and Antimicrobial Activities of a Schiff Base Derived from Acetyl Acetone and 2-aminopyridine and its Cobalt (II) and Nickel (II) Complexes. *Journal of Basics and Applied Sciences Research (JOBASR)*, 3(2), 62–69. <https://doi.org/https://dx.doi.org/10.4314/jobasr.v3i2.7>
- Rajasekar, M., Mary, J., Sivakumar, M., Ravichandran, S. S., & Srinivasan, D. (2025). Recent advances in organic fluorophore-based Schiff base metal complexes:

Applications in biomedicine and related fields. In *Results in Chemistry* (Vol. 15). <https://doi.org/10.1016/j.rechem.2025.102166>

Sandhu, Q. U. A., Pervaiz, M., Majid, A., Younas, U., Saeed, Z., Ashraf, A., Khan, R. R. M., Ullah, S., Ali, F., & Jelani, S. (2023). Review: Schiff base metal complexes as anti-inflammatory agents. In *Journal of Coordination Chemistry* (Vol. 76, Issues 9–10). <https://doi.org/10.1080/00958972.2023.2226794>

Senthil Kumar Raju, Archana Settu, Archana Thiyagarajan, Divya Rama, Praveen Sekar, & Shridharshini Kumar. (2022). Biological applications of Schiff bases: An overview. *GSC Biological and Pharmaceutical Sciences*, 21(3). <https://doi.org/10.30574/gscbps.2022.21.3.0484>

Sharma, P., Reddy, P. K., & Kumar, B. (2021). Trace Element Zinc, a Nature's Gift to Fight Unprecedented Global Pandemic COVID-19. In *Biological Trace Element Research* (Vol. 199, Issue 9). <https://doi.org/10.1007/s12011-020-02462-8>

Sheokand, S., Mohite, M. A., Mondal, D., Rangarajan, S.,

& Balakrishna, M. S. (2023). 1,2,3-Triazolyl bisphosphine with pyridyl functionality: synthesis, copper(i) chemistry and application in click catalysis. *New Journal of Chemistry*, 47(28). <https://doi.org/10.1039/d3nj01445b>

Singh, A., Gogoi, H. P., Barman, P., Das, A., & Pandey, P. (2022). Tetracoordinated ONNO donor purine-based Schiff base and its metal complexes: Synthesis, characterization, DNA binding, theoretical studies, and bioactivities. *Applied Organometallic Chemistry*, 36(10). <https://doi.org/10.1002/aoc.6852>

Vafazadeh, R., & Bagheri, M. (2015). Kinetics and Mechanism of the Ligand Exchange Reaction Between Tetradentate Schiff Base N,N'-ethylen-bis(salicylaldimine) and Ni(N,N'-propylen-bis(salicylaldimine)). *S. Afr. J. Chem.*, 68, 21–26. <https://doi.org/http://dx.doi.org/10.17159/0379-4350/2015/v68a4>